Journal of Mathematical Chemistry 14 (1993) 427–450

Distance functions as generators of chirality measures

Noham Weinberg

Department of Chemistry, Simon Fraser University, Burnaby, British Columbia, Canada V5A 1S6

Kurt Mislow

Department of Chemistry, Princeton University, Princeton, NJ 08544, USA

Received 8 March 1993

A non-numerical analysis is presented of chirality measures associated with a set of topologically equivalent distance functions. A chirality measure is defined as the minimum distance that separates a chiral and an achiral object (first kind) or two enantiomorphs (second kind). On the basis of this analysis, as applied to triangles in the Euclidean plane, results of an earlier computational study of the Hausdorff chirality measure are now fully understood. Analytical proof has been provided for an earlier conjecture, based on a numerical analysis, that the union of enantiomorphous triangles is achiral under conditions of maximal overlap. Geometric parameters for the most chiral triangle, as determined by a family of three measures of the first kind, are found to differ substantially from those determined by the corresponding measures of the second kind; none of these extremal triangles is degenerate.

1. Introduction

It has been recognized [1] that measures designed to quantify chirality fall into two classes: those that gauge the extent to which a chiroid differs from an achiral reference object (measures of the first kind) and those that gauge the extent to which two enantiomorphs differ from one another (measures of the second kind). Among the latter, the Hausdorff chirality measure [1,2] was singled out as the general method of choice because of its broad applicability, which extends to objects that are embedded in higher-dimensional spaces, such as one- or two-dimensional objects in Euclidean 3-space (E^3) or one-dimensional objects in the plane (E^2), and to continuous as well as to discrete sets (with the latter representing, in a chemical context, the array of nuclear positions in a rigid molecular model).

The Hausdorff distance $h(Q, Q')$ between two sets Q and Q' is the smallest number δ that has the following two properties: i) a spherical ball of radius δ cen-

tered at any point of Q contains at least one point of Q', and ii) a spherical ball of radius δ centered at any point of Q' contains at least one point of Q. The Hausdorff chirality measure $f(Q)$ for enantiomorphous sets Q and Q' is given by eq. (1), where $h_{min}(Q, Q')$ corresponds to the position of optimal (i.e., maximal) overlap and the diameter $d(Q)$ is the largest distance between any two points in Q.

$$f(Q) = h_{min}(Q, Q')/d(Q) . \tag{1}$$

This measure, which provides a numerical value for the degree of chirality of Q, is similarity-invariant, normalized in the interval [0,1], and zero if and only if Q is achiral. The diameter may be assigned unit length without loss of generality; eq. (1) then reduces to eq. (2):

$$f(Q) = h_{min}(Q, Q') . \tag{2}$$

In previous studies [1,2], the degree of chirality of triangles and tetrahedra, represented as physical objects in E^3 consisting of unit masses centered at the three and four vertices, respectively, was determined by a numerical method in which a multidimensional hypersurface was explored by standard computational means: different superimpositions of Q and Q', obtained by translation–rotation of one enantiomorph relative to the other, led to the global minimum and hence to an estimate of $f(Q)$. In the present paper we show that the salient results of these studies can be rationalized in light of a non-numerical analysis, that other distance functions (metrics) are capable of yielding results similar to those obtained in our previous work, and that measures of the first kind can be developed for each of these metrics, including the Hausdorff measure. For reasons of convenience and simplicity, we have restricted our analysis to triangles in E^2, represented by vertices as sets of points.

Underlying all chirality measures χ is the concept of a distance, either one between a chiral and an achiral object (first kind), or one between two enantiomorphs (second kind). A relevant class of distance functions is defined by eq. (3) (see [3]):

$$D_p(d_A, d_B, d_C) = (d_A^p + d_B^p + d_C^p)^{1/p} , \tag{3}$$

where d_A, d_B, d_C denote the distances from the vertices A, B, C of a given triangle to the nearest (neighboring) vertices of the enantiomorph or to the nearest vertices of an achiral reference object. The associated chirality measure is given by eq. (4):

$$\chi_p = \min\{D_p(d_A, d_B, d_C)\} . \tag{4}$$

A family of topologically equivalent metrics may be derived from eq. (3). For $p = 1$ and $p = 2$, eq. (5) and (6) apply:

$$D_1(d_A, d_B, d_C) = d_A + d_B + d_C , \tag{5}$$

$$D_2(d_A, d_B, d_C) = (d_A^2 + d_B^2 + d_C^2)^{1/2} . \tag{6}$$

As $p \to \infty$, $D_p(d_A, d_B, d_C)$ converges to $D_\infty(d_A, d_B, d_C)$. It is easily seen that if, for example, $d_A \geqslant d_B, d_C$

$$D_\infty(d_A, d_B, d_C) = \lim_{p \to \infty} D_p(d_A, d_B, d_C) = d_A . \tag{7}$$

Hence,

$$D_\infty(d_A, d_B, d_C) = \max\{d_A, d_B, d_C\} . \tag{8}$$

The Hausdorff distance $h(Q, Q')$ is therefore seen to be a special case (eq. (8)) in the class represented by eq. (3). In what follows we analyze chirality measures of both kinds for different metrics D_p.

2. Chirality measures χ_p'' of the second kind

Given a normalized triangle, a chirality measure χ_p'' of the second kind is defined, according to eq. (4), as the global minimum of function (3), calculated at the optimum superimposition of the enantiomorphs. For a triangle ABC (with sides $a < b < c = 1$) and its enantiomorph $A'B'C'$, there exist only three possible classes of arrangements of vertices, and hence only three classes of optimum superimpositions.

Class I: At least two vertices of a given triangle share the same nearest neighboring vertex of the enantiomorph. Of all possible arrangements of this type, the minimum distance is reached when vertices A and A' with the smallest angle are placed on the shortest sides, $B'C'$ and BC, respectively (fig. 1). Any change in the mutual position of the two triangles that displaces A or A' out of the respective side will increase the distances between vertices, and hence the distance D_p. The particular optimum position of the vertex on the side depends on the choice of the D_p metric,

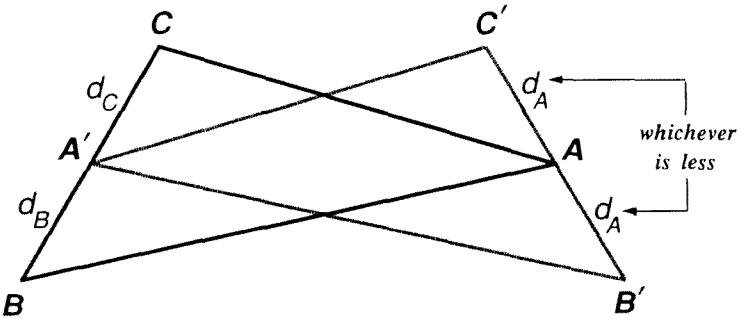

Fig. 1.

but in all cases the position of A on $B'C'$ is the same as (i.e. mirrors) that of A' on BC. Therefore, in optimum superimpositions of this type, the unions of enantiomorphs have axial symmetry, and are thus achiral.

Class II: Each vertex of a given triangle has only one nearest neighboring vertex of the enantiomorph which is its equivalent (fig. 2). For this class of superimpositions, D_p is determined by the distances between three pairs of equivalent vertices: A–A', B–B', C–C'. Of all possible arrangements of this type, the minimum distance is reached when links AA', BB' and CC' are parallel to each other. Any shift of one of the component triangles in the orthogonal direction simultaneously stretches all links and hence increases D_p. This superimposition is obviously achiral, with the symmetry axis orthogonal to the links and passing through their midpoints.

Class III: Similar to class II, but with one equivalent and two nonequivalent vertices as nearest neighbors (fig. 3). Depending on which is the equivalent pair, we have three subclasses:

(IIIA) A–B', B–A', C–C';
(IIIB) A–A', B–C', C–B';
(IIIC) A–C', B–B', C–A'.

A rough estimate of the minimum value of the function D_p for class IIIA can be obtained from the superimposition of enantiomorphs shown in fig. 4. As seen from this figure, $d_A = d_B = b - a$ and $d_C = 0$. Substitution in eq. (3) yields

$$D_p^{IIIA} \approx 2^{1/p}(b - a) \tag{9}$$

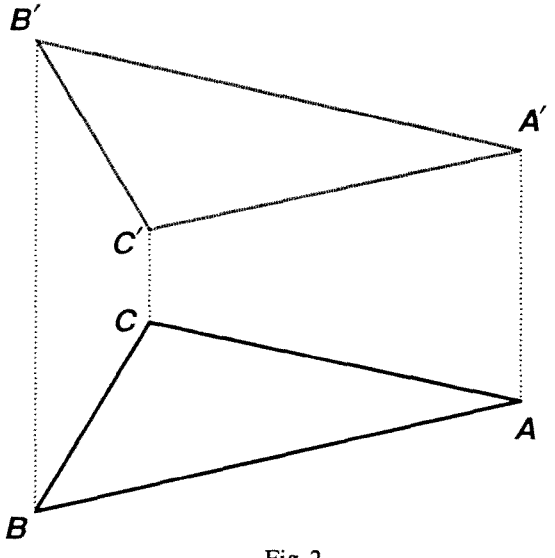

Fig. 2.

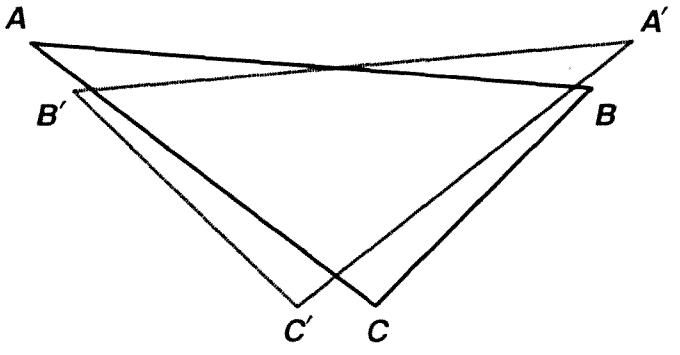

Fig. 3.

and since $\lim_{p\to\infty} 2^{1/p} = 1$

$$D_{\infty}^{IIIA} \approx b - a. \tag{10}$$

Similarly, for class IIIB we have

$$D_{p}^{IIIB} \approx 2^{1/p}(c - b), \tag{11}$$

$$D_{\infty}^{IIIB} \approx c - b, \tag{12}$$

and for class IIIC

$$D_{p}^{IIIC} \approx 2^{1/p}(c - a), \tag{13}$$

$$D_{\infty}^{IIIC} \approx c - a. \tag{14}$$

Note that, in the chosen convention, D_p^i connotes the minimum value of D_p for class i. As seen from eq. (9)–(14), class IIIC can be neglected, since $c > b > a$, and hence $c - a > c - b$ and $c - a > b - a$.

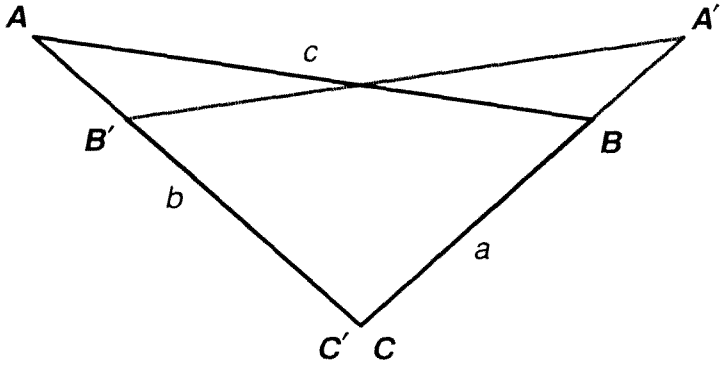

Fig. 4.

Though the very existence of classes I-III is determined by the mutual arrangement of the vertices of the enantiomorphs, the particular optimum superimpositions of the enantiomorphs and the specific values of chirality measures depend on the choice of the D_p metrics, and are discussed below, starting with the Hausdorff measure.

2.1. HAUSDORFF MEASURE χ''_∞

2.1.1. Optimum superimposition for classes I and II

For optimum superimpositions in class I, vertex A' lies on side BC. This means that the sum $d_B + d_C = a$ (see fig. 1), and hence the minimum of function D_∞ (eq. (8)) is reached at

$$d_A = d_B = d_C = a/2\,, \tag{15}$$

i.e., when vertices A and A' are positioned at the midpoints of sides $B'C'$ and BC, respectively. Any other superimposition will increase at least one of the d's and hence D_∞. Substitution of eq. (15) into eq. (8) gives

$$D^{I}_{\infty} = a/2 \tag{16}$$

as the minimum distance for class I.

In class II, the minimum of D_∞ corresponds to a superimposition in which the longest sides, AB and $A'B'$, of the enantiomorphs are parallel, vertices C and C' lie on $A'B'$ and AB, respectively, and links AA', BB', and CC' are orthogonal to AB and $A'B'$ (fig. 5). In this case

$$d_A = d_B = d_C = h_C\,,$$

where h_C is the smallest height of the triangle. Hence

$$D^{II}_{\infty} = h_C\,. \tag{17}$$

Any other superimposition will increase one of the d's and hence D_∞.

2.1.2. Chirality map of the shape space

It has been shown [4] that all normalized, chirally related (i.e., homochiral) triangles can be represented in a construction in which two vertices, A and B, are located at $(1/2, 0)$ and $(-1/2, 0)$, respectively, while the third, $C\,(x, y)$, maps into the region bounded on two sides by coordinate axes and on the third by the arc of the

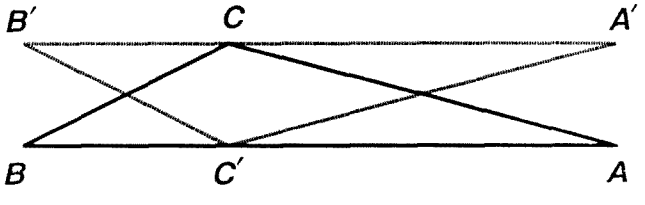

Fig. 5.

circle centered at point A (fig. 6). Region OBR of the coordinate plane forms a *shape space*, every internal point of which represents a unique chiral triangle. Boundaries BR and OR represent achiral triangles, boundary BO represents degenerate triangles with three collinear vertices, and point R $(0, \sqrt{3}/2)$ represents the regular triangle.

Given a chiral triangle, four different equations, (10), (12), (16), and (17), can be used to calculate the minimum distances D^i_∞ between enantiomorphs. According to eq. (4), the chirality measure χ''_∞ is the smallest of the four D^i_∞'s:

$$\chi''_\infty = \min\{D^I_\infty, D^{II}_\infty, D^{IIIA}_\infty, D^{IIIB}_\infty\}.$$

One may therefore anticipate four subspaces in the shape space:

Region I: $\chi''_\infty = D^I_\infty$.
Region II: $\chi''_\infty = D^{II}_\infty$.
Region IIIA: $\chi''_\infty = D^{IIIA}_\infty$.
Region IIIB: $\chi''_\infty = D^{IIIB}_\infty$.

The interregion boundaries are defined by the condition of equality for the respective D^i_∞'s. Thus, for the I/II boundary, equating D^I_∞ (eq. (16)) and D^{II}_∞ (eq. (17)) gives

$$a/2 = h_C.$$

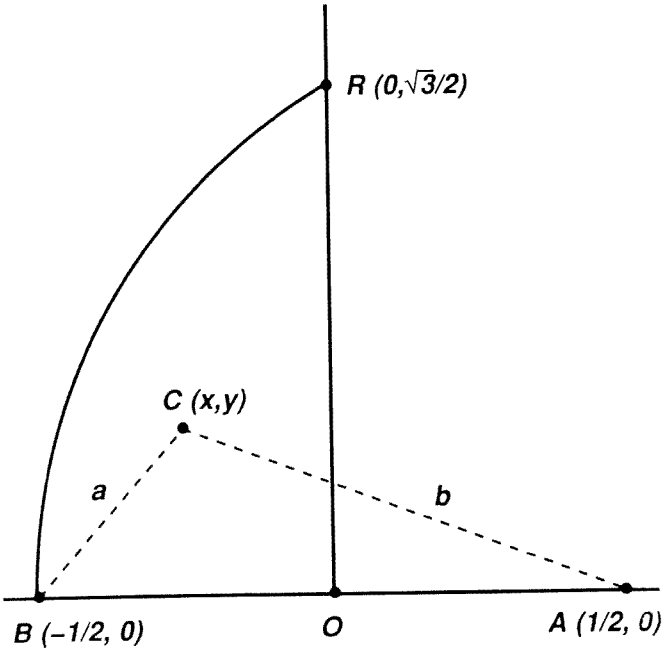

Fig. 6.

Taking into account that, as seen from fig. 6,

$$a = [(1/2 + x)^2 + y^2]^{1/2}$$

and

$$h_C = y,$$

one obtains the following equation for the I–II boundary line:

$$y = (x + 1/2)/\sqrt{3}.$$

This is a straight line that passes through point B $(-1/2, 0)$ and forms an angle of 30° with the x axis.

Similarly one can derive analytical equations for the remaining boundary lines. The resulting diagram, showing the four regions of the shape space, is presented in fig. 7. Fig. 8 shows the chirality map of the shape space. The contour lines represent equally spaced levels of constant chirality χ. As follows from eqs. (10), (12), (16), and (17), these are

Region I: arcs of circles centered at point B

$$(x + 1/2)^2 + y^2 = (2\chi)^2.$$

Region II: horizontal lines

$$y = \chi.$$

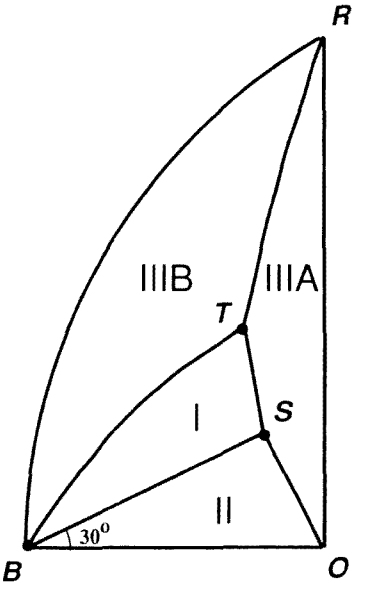

Fig. 7.

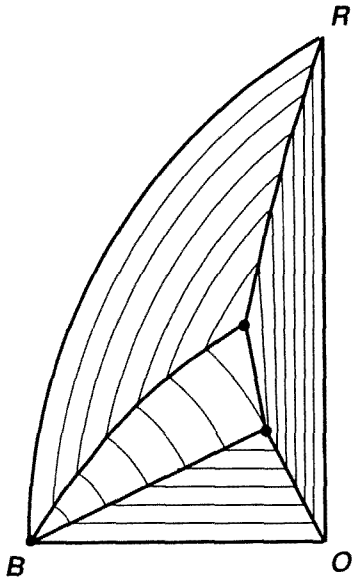

Fig. 8.

Region IIIA: arcs of hyperbolas with foci at points B and A

$$\frac{x^2}{(\chi/2)^2} - \frac{y^2}{1/4 - (\chi/2)^2} = 1 .$$

Region IIIB: arcs of circles centered at point A

$$(x - 1/2)^2 + y^2 = (1 - \chi)^2 .$$

If fig. 8 is seen as the projection of a three-dimensional map, the boundary lines may be thought of as ridges that represent triangles with a relatively high degree of chirality. These ridges separate valleys (regions) of relatively low chirality, and the degree of chirality along the ridges increases from the corners of the map (points O, B, and R) toward the center (points S and T in fig. 7). These results serve to rationalize a previously unexplained observation. In our earlier work [1] we had computed the Hausdorff chirality measure $f(Q)$ for triangles, over the whole of the shape space, on a 0.02 unit grid along the x and y axes. The values of the function were represented as a density plot by different shadings, with darker shadings indicating higher values. An examination of the published plot (fig. 5 in [1]) reveals the faint presence of dark streaks leading from the corners of the map to the center. Fig. 9 displays the same map at higher density, on a 0.005 unit grid. The dark streaks are now clearly displayed. Comparison between fig. 8 and 9 shows that the heretofore unexplained high-density streaks match the boundary lines calculated in the present work.

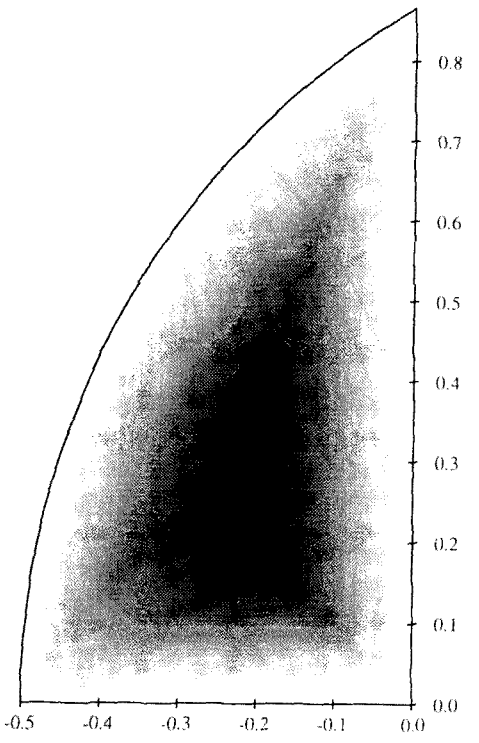

Fig. 9.

The maps in fig. 7 and 8 show the existence of three triple points, T, S, and B, at the junctures of three regions. The point at B represents a degenerate isosceles triangle ($b = c, a = 0$). The point at T has the highest degree of chirality and hence represents the most chiral triangle. One can roughly estimate the parameters of this triangle from the condition (triple point of I, IIIA, IIIB):

$$D_{\infty}^{I} = D_{\infty}^{IIIA} = D_{\infty}^{IIIB}.$$

From eq. (10), (12), and (16) it follows that

$$a/2 \approx b - a \approx 1 - b.$$

Hence $a \approx 1/2$ and $b \approx 3/4$;
and $\alpha \approx 29°, \beta \approx 47°, \gamma \approx 104°; \chi''_{\infty} \approx 0.25$.

The exact parameters for this triangle are reported in section 2.1.4.

2.1.3. Symmetry of the union of enantiomorphs in their optimum superimposition

As mentioned above, the union of the enantiomorphs in their optimum superimpositions for classes I and II (fig. 1 and 5) has axial symmetry. In order to prove the same for class III, we start with the superimposition of fig. 4. This is not an optimum superimposition yet, since we can decrease the distances between nonequiva-

lent vertices, BA' and $B'A$, by increasing the distance CC' until they become equal (fig. 3):

$$d_A = d_B = d_C . \tag{18}$$

Three parameters now define the superimposition: the CC' link length, L, and two rocking angles, θ and θ' (fig. 10). As seen from fig. 10,

$$d_A^2 = (AB')^2 = a^2 + b^2 + L^2 + 2ab\ \cos(\gamma + \theta + \theta') + 2L[b\ \cos(\gamma + \theta') + a\ \cos\ \theta], \tag{19}$$

$$d_B^2 = (BA')^2 = a^2 + b^2 + L^2 + 2ab\ \cos(\gamma + \theta + \theta') + 2L[b\ \cos(\gamma + \theta) + a\ \cos\ \theta'], \tag{20}$$

$$d_C = (CC') = L . \tag{21}$$

Subtracting eq. (19) from eq. (20) and taking into account condition (18), we have

$$d_B^2 - d_A^2 = 4L\ \sin\frac{\theta - \theta'}{2}\left[b\ \sin\left(\gamma + \frac{\theta + \theta'}{2}\right) + a\ \sin\frac{\theta + \theta'}{2}\right] = 0 . \tag{22}$$

Eq. (22) has two solutions

$$\theta = \theta' \tag{23}$$

and

$$\theta = -\theta' - \arctan\frac{b\ \sin\ \gamma}{b\ \cos\ \gamma + a} .$$

The first of these corresponds to smaller values of d_B and d_A and hence is the solution of choice.

It is obvious from fig. 10 that, under condition (23), the union of enantiomorphs has axial symmetry.

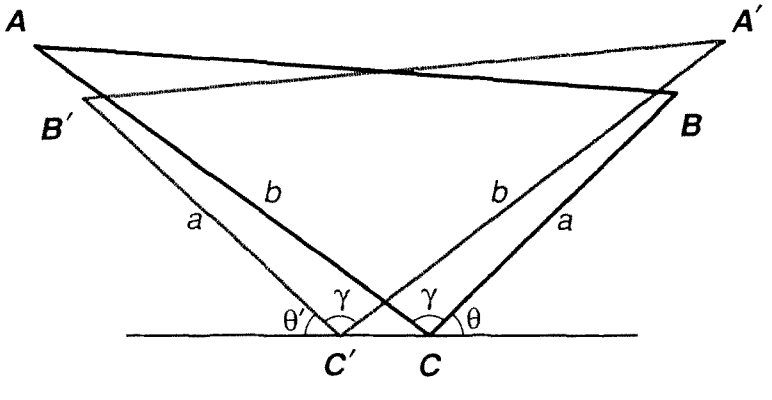

Fig. 10.

In our previous, computational exploration of the shape space for triangles [1], it was found that three different optimized superimpositions of the most chiral triangle and its enantiomorph yielded the same value of $f(Q)$ (eq. (2)) within the error limits of the calculation. It was also observed that, in all three orientations, a line of reflection passes through the region of overlap (fig. 6 in [1]); that is, all three orientations have axial symmetry. Both observations are now fully understood. First, the three different orientations correspond to the three classes of superimpositions whose regions meet at T in fig. 7; specifically, with reference to fig. 6 in [1], the orientations depicted at the top left, top right, and bottom of that figure correspond to superimpositions of types IIIA, IIIB, and I, respectively. Second, the proof herein presented that, under conditions of optimal overlap, superimpositions in classes III and I yield achiral unions rationalizes the previously observed numerical results.

2.1.4. Optimum superimposition for class III and the exact solution for the most chiral triangle

It is seen from eq. (19) and (20) that $d_A = d_B$ at any $L = d_C$ and $\theta = \theta'$. In order to find the optimum solution we have to find the minimum d_A with respect to θ at a given d_C and then put it equal to d_C.

Differentiation of eq. (19) with $\theta = \theta'$ gives

$$2ab\ \sin(\gamma + 2\theta) + L[b\ \sin(\gamma + \theta) + a\ \sin\ \theta] = 0\,. \tag{24}$$

At the same time, condition (18), in combination with eq. (21) and (23), reduces (19) to

$$a^2 + b^2 + 2ab\ \cos(\gamma + 2\theta) + 2L[b\ \cos(\gamma + \theta) + a\ \cos\ \theta] = 0\,. \tag{25}$$

Eq. (24) and (25) determine the optimum values of θ and L. L can be excluded from these equations to give eq. (26):

$$\frac{4ab\ \sin(\gamma + 2\theta)}{b\ \sin(\gamma + \theta) + a\ \sin\ \theta} = \frac{a^2 + b^2 + 2ab\ \cos(\gamma + 2\theta)}{b\ \cos(\gamma + \theta) + a\ \cos\ \theta}\,, \tag{26}$$

which can be easily reduced to a cubic equation in $\tan\theta$. The optimum θ thus found can then be substituted in eq. (24) to give L. By virtue of (8), (18), and (21), D_∞^{IIIA} is equal to this optimum L, and hence eq. (24) can be rewritten as

$$D_\infty^{IIIA} = -\frac{2ab\ \sin(\gamma + 2\theta)}{b\ \sin(\gamma + \theta) + a\ \cos\ \theta}\,. \tag{27}$$

Together with eq. (26), eq. (27) determines the exact solution for D_∞^{IIIA} in the region IIIA. Similarly,

$$D_\infty^{IIIB} = -\frac{2bc\ \sin(\alpha + 2\theta)}{c\ \sin(\alpha + \theta) + b\ \cos\ \theta}\,, \tag{28}$$

$$\frac{4bc\ \sin(\alpha+2\theta)}{c\ \sin(\alpha+\theta)+b\ \sin\ \theta}=\frac{b^2+c^2+2bc\ \cos(\alpha+2\theta)}{c\ \cos(\alpha+\theta)+b\ \cos\ \theta}\,. \tag{29}$$

We use eq. (16), (17), (26)–(29) to find the most chiral triangle in the D_∞ metric (T in fig. 7): $\alpha = 21.02°, \beta = 43.69°, \gamma = 115.29°, \chi''_\infty = 0.1983$. The calculated parameters are in excellent agreement with the earlier numerical solution ([1]): $\alpha \approx 21.5°, \beta \approx 44.2°, \gamma \approx 114.3°$, $f(Q) = 0.196, 0.197, 0.201$ for the three orientations in fig. 6 of [1]. For completeness we note that the chiral triangle represented by triple point S in fig. 7 has the following parameters: $\alpha = 14.75°$, $\beta = 30.00°$, $\gamma = 135.25°, \chi_\infty = 0.1808$.

2.2. EUCLIDEAN MEASURE χ''_2

2.2.1. Optimum superimpositions for classes I and II

In this case condition (15) is no longer valid and we need to find the optimum superimposition by direct minimization of the distance function (6). As is seen from fig. 1, there are two equivalent solutions for class I that give the same value of the D_2 distance, namely

$$d_A = d_B < d_C = a - d_A$$

and

$$d_A = d_C < d_B = a - d_A\,. \tag{30}$$

Substituting (30) into (6) we have

$$[D_2(d_A)]^2 = 2d_A^2 + (a - d_A)^2\,. \tag{31}$$

Differentiation of (31) gives the following expression for the optimum value of d_A:

$$d_A = a/3\,,$$

which, substituted into (31), gives

$$D_2^I = a\sqrt{2/3}\,. \tag{32}$$

One can proceed in similar fashion with the case of class II. As mentioned above, links AA', BB', and CC' are parallel in the optimum superimposition of this class, and hence, as seen from fig. 11, two parameters completely determine their lengths, the tilt angle ϕ, and the shift parameter $z = \pm d_B$ (we choose $z = +d_B$ if B is placed above B', and $z = -d_B$ in the opposite case):

$$\begin{aligned} d_A &= |z - 2c\ \sin\ \phi|\,,\\ d_B &= |z|\,,\\ d_C &= |z + 2a\ \sin(\beta - \phi)|\,. \end{aligned} \tag{33}$$

This makes distance D_2 (eq. (6)) a function of two variables, z and ϕ. Differentia-

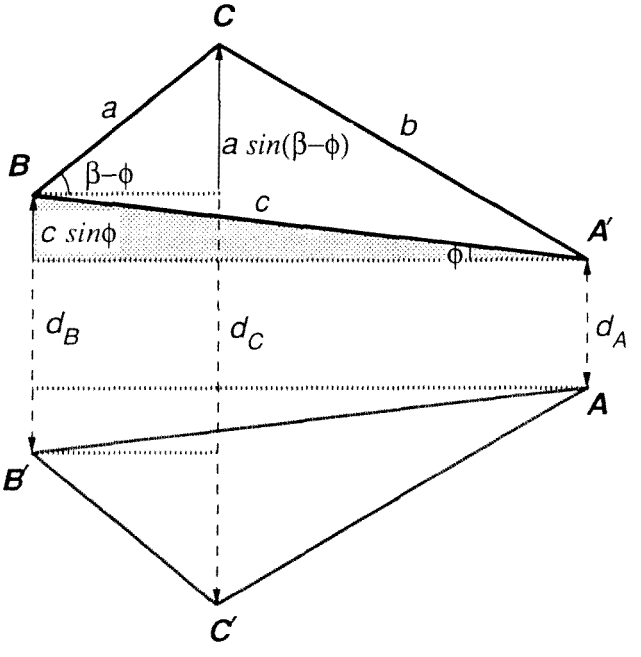

Fig. 11.

tion of D_2 with respect to these variables gives for the optimum superimposition of class II:

$$\begin{aligned} d_A &= \tfrac{2}{3}|a \sin(\beta - \phi) + 2c \sin \phi|, \\ d_B &= \tfrac{2}{3}|a \sin(\beta - \phi) - c \sin \phi|, \\ d_C &= \tfrac{2}{3}|2a \sin(\beta - \phi) + c \sin \phi|, \end{aligned} \tag{34}$$

$$\tan 2\phi = \frac{a \sin \beta(2a \cos \beta - c)}{c^2 - ac \cos \beta + a^2 \cos \beta}. \tag{35}$$

The minimum distance D_2^{II} for class II can be calculated from (34) and (35) by use of eq. (6). A simple estimate of the upper bound for D_2^{II} can be obtained if one neglects the tilt and calculates the minimum D_2 at $\phi = 0$. It follows from (34) that in this case

$$d_A = d_B = \tfrac{1}{2}d_C = \tfrac{2}{3}a \sin \beta = \tfrac{2}{3}h_C,$$

which, substituted into eq. (6), gives

$$D_2^{II} \leqslant 2h_C\sqrt{2/3}. \tag{36}$$

D_2^{II} reaches its upper bound (36) if $\phi = 0$, which, according to eq. (35), corresponds to isosceles triangles with $a = b$ and $c = 2a \cos \beta$.

2.2.2. Chirality map of the shape space

Here, as in the case of the Hausdorff measure, we have four regions in the shape space, depending on which of the four minima, D_2^{I}, D_2^{II}, D_2^{IIIA} or D_2^{IIIB}, is the global one. According to eqs. (9)–(12), (16), (17), (32), and (36), D_2^{i} and D_∞^{i} are related by

$$D_2^{I} = \sqrt{8/3}\, D_\infty^{I},$$

$$D_2^{II} \approx \sqrt{8/3}\, D_\infty^{II},$$

$$D_2^{III} \approx \sqrt{2}\, D_\infty^{III}, \tag{37}$$

and hence

$$\chi_2'' \approx \sqrt{8/3}\, \chi_\infty'' \quad \text{(in regions I and II)},$$
$$\chi_2'' \approx \sqrt{2}\, \chi_\infty'' \quad \text{(in regions IIIA and IIIB)}. \tag{38}$$

It follows from eqs. (37) and (38) that the positions of the interregion boundaries (see fig. 7) are roughly the same for χ_2'' and χ_∞''.

2.2.3. Symmetry of the union of enantiomorphs in their optimum superimposition

Here, as in the case of the D_∞ metric, we only need to consider optimum superimpositions for class III. We start again with fig. 10 and eqs. (19)–(21). Substituting these equations into (6) gives D_2 as a function of CC' link length L and rocking angles θ and θ'. In the optimum superimposition, partial derivatives with respect to these parameters equal zero, which results in the following set of equations:

$$2ab\, \sin(\gamma+\theta+\theta') + L[b\, \sin(\gamma+\theta) + a\, \sin\, \theta] = 0, \tag{39}$$

$$2ab\, \sin(\gamma+\theta+\theta') + L[b\, \sin(\gamma+\theta') + a\, \sin\, \theta'] = 0, \tag{40}$$

$$3L + b\, \cos(\gamma+\theta) + b\, \cos(\gamma+\theta') + a\, \cos\, \theta + a\, \cos\, \theta' = 0. \tag{41}$$

Subtracting eq. (40) from eq. (39) yields

$$\sin\frac{\theta-\theta'}{2}\left[b\, \cos\left(\gamma+\frac{\theta+\theta'}{2}\right) + a\, \cos\frac{\theta+\theta'}{2}\right] = 0. \tag{42}$$

Eq. (42) has two solutions

$$\theta = \theta'$$

and

$$\theta = -\theta' + \arctan\frac{b\, \cos\, \gamma + a}{b\, \sin\, \gamma}.$$

The first of these corresponds to the minimum of the function D_2 and hence is the solution of choice. Thus, the union of enantiomorphs in the D_2-optimum superimposition has axial symmetry.

2.2.4. Optimum superimposition for class III and the exact solution for the most chiral triangle

With condition $\theta = \theta'$ in mind, eqs. (39)–(41) can be rearranged into

$$L = -\tfrac{2}{3}[b\ \cos(\gamma+\theta) + a\ \cos\ \theta]\,, \tag{43}$$

$$3ab\ \sin(\gamma+2\theta) - [b\ \cos(\gamma+\theta) + a\ \cos\ \theta][b\ \sin(\gamma+\theta) + a\ \sin\ \theta] = 0\,. \tag{44}$$

Eq. (44) transforms into a quadratic equation in tan θ. The optimum θ thus found, through eqs. (43), (19)–(21) and then (6), determines the exact solution for D_2^{IIIA}. Similarly one can calculate D_2^{IIIB}.

We applied this scheme to find the most chiral triangle for measure χ_2''. The obtained parameters are listed in table 1 and are practically the same as for the Hausdorff measure χ_∞''.

2.3. MEASURE χ_1''

2.3.1. Optimum superimpositions for classes I and II

Substitution of eq. (30) into (5) gives for a superimposition of class I (fig. 1)

$$D_1(d_A) = d_A + a\,,$$

from which it follows that the minimum value

$$D_1^I = a \tag{45}$$

is reached at $d_A = 0$, i.e., when vertex A is superposed on either B' or C'.

Similarly, it follows from eqs. (5) and (33) that for a superimposition of class II (fig. 11)

$$D_1(z,\phi) = |z - 2c\ \sin\ \phi| + |z| + |z + 2a\ \sin(\beta - \phi)|\,. \tag{46}$$

Table 1
Degree of chirality χ and geometric parameters for the most chiral triangle as determined by measures of the first and second kind.

	Measure		Parameters of the most chiral triangle (deg)		
Kind	Distance function	χ_{max}	α	β	γ
Second	D_∞	0.1983	21.02	43.69	115.29
	D_2	0.3261	21.16	43.46	115.38
	D_1	0.4304	24.29	48.58	107.13
First	D_∞	0.1067	16.43	37.65	125.93
	D_2	0.1724	16.90	37.35	125.35
	D_1	0.2320	17.59	40.88	121.53

Function (46) reaches its minimum value

$$D_1^{II} = 2a \sin \beta = 2h_C \tag{47}$$

at $\phi = 0$ and $z = 0$, i.e., when vertices A and B are superposed on vertices A' and B', respectively.

2.3.2. Chirality map of the shape space

It follows from eqs. (9)–(12), (16), (17), (45), and (47) that

$$D_1^i \approx 2D_\infty^i$$

and hence

$$\chi_1'' \approx 2\chi_\infty'' .$$

This means that measure χ_1'' should produce basically the same chirality map as χ_∞''.

2.3.3. Symmetry of the union of enantiomorphs in their optimum superimposition

Substitution of eqs. (19)–(21) into eq. (5) gives D_1 as a function of parameters L, θ, and θ'. Differentiation with respect to these parameters yields the following equations for the optimum superimposition of class III:

$$(1/d_A + 1/d_B)ab \sin(\gamma + \theta + \theta') + \frac{La}{d_A} \sin \theta + \frac{Lb}{d_B} \sin(\gamma + \theta) = 0 , \tag{48}$$

$$(1/d_A + 1/d_B)ab \sin(\gamma + \theta + \theta') + \frac{Lb}{d_A} \sin(\gamma + \theta') + \frac{La}{d_B} \sin \theta' = 0 . \tag{49}$$

Subtraction of eq. (49) from eq. (48) yields

$$b\left[\frac{\sin(\gamma + \theta)}{d_B} - \frac{\sin(\gamma + \theta')}{d_A}\right] + a\left[\frac{\sin \theta}{d_A} - \frac{\sin \theta'}{d_B}\right] = 0 .$$

The solution $\theta = \theta'$ corresponds to the minimum D_1, and the corresponding superimposition obviously has axial symmetry.

2.3.4. Optimum superimposition for class III and the exact solution for the most chiral triangle.

We start with the case of $L = 0$. Under this condition eqs. (48)–(49) give an optimum θ of

$$\theta = \frac{\pi}{2} - \frac{\gamma}{2} , \tag{50}$$

which corresponds to the superimposition in fig. 4, where d_A is merely

$$d_A = b - a . \tag{51}$$

Differentiation of D_1 with respect to L gives

$$\frac{dD_1}{dL} = \frac{2}{d_A}[L + b\ \cos(\gamma + \theta) + a\ \cos\ \theta] + 1\,. \tag{52}$$

According to (50) and (51), at $L = 0$ and optimum θ this derivative equals

$$\left.\frac{dD_1}{dL}\right|_{L=0} = 1 - 2\ \sin\frac{\gamma}{2}\,. \tag{53}$$

It follows from eq. (53) that the sign of the derivative is crucially dependent on the parameter γ. For class IIIB, according to our definition of the shape space (section 2.1.2.), this parameter cannot exceed 60°, and hence the derivative is positive. This means that the superimposition in fig. 4 is optimum in class IIIB since any increase in L will increase D_1. In other words, an approximate solution (11) is the accurate one for the D_1 metric.

The situation is different for class IIIA, where $60° < \gamma < 180°$, and hence the derivative (53) is always negative. This means that D_1 will benefit from reducing two distances d_A and d_B at the expense of L. In order to find an exact solution for this case, we put derivative (52) equal to zero, which gives

$$d_A = -2[L + b\ \cos(\gamma + \theta) + a\ \cos\ \theta]\,. \tag{54}$$

Substitution into eq. (19) yields

$$a\ \sin\ \theta - b\ \sin(\gamma + \theta) = \sqrt{3}\,[L + b\ \cos(\gamma + \theta) + a\ \cos\ \theta]\,. \tag{55}$$

At $\theta = \theta'$, eqs. (48) and (49) transform into eq. (24) which, combined with eq. (55), gives the following equation for an optimum θ:

$$[b\ \sin(\gamma + \theta) - a\ \sin\ \theta][\sqrt{3}\ b\ \cos(\gamma + \theta) - \sqrt{3}\ a\ \cos\ \theta + b\ \sin(\gamma + \theta) + a\ \sin\ \theta] = 0. \tag{56}$$

Eq. (56) has two roots, corresponding to a minimum and maximum D_1, respectively. The minimum D_1 root represents the case where the first bracket in eq. (56) equals zero. According to eqs. (54) and (55), this is the limiting case of $d_A = d_B = 0$, where vertices *A* and *B* are superposed on vertices *B'* and *A'*, respectively. The minimum value of D_1 equals the *CC'* distance L and can be found as

$$D_1^{IIIA} = \frac{b^2 - a^2}{c}\,. \tag{57}$$

Eqs. (11), (45), (47), and (57) were used to calculate the parameters of the most chiral triangle in the D_1 metric. The results obtained are presented in table 1.

2.4. GENERAL CASE: MEASURE χ_p''

2.4.1. Optimum superimposition for classes I and II

Substitution of eq. (30) into eq. (3) gives for a superposition of class I

$$[D_p(d_A)]^p = 2d_A^p + (a - d_A)^p\,,$$

from which it follows that the minimum value of

$$D_p^I = a(1 + 2^{1/(1-p)})^{(1-p)/p} \tag{58}$$

is reached at $d_A = a/(2^{1/(p-1)} + 1)$.

In order to estimate an upper bound for D_p^{II} we assume $\phi = 0$ in eq. (33). Under this assumption

$$[D_p(d_A)]^p = 2d_A^p + (2h_C - d_A)^p$$

for a superimposition of class II, from which it follows that

$$D_p^{II} \leqslant (1 + 2^{1/(1-p)})^{(1-p)/p} \cdot 2h_C . \tag{59}$$

2.4.2. Chirality map of the shape space

It follows from eqs. (9)–(12), (16), (17), (58), and (59) that

$$\begin{aligned} D_p^I &= 2(1 + 2^{1/(1-p)})^{(1-p)/p} \cdot D_\infty^I , \\ D_p^{II} &\approx 2(1 + 2^{1/(1-p)})^{(1-p)/p} \cdot D_\infty^{II} , \\ D_p^{III} &\approx 2^{1/p} \cdot D_\infty^{III} , \end{aligned} \tag{60}$$

and hence

$$\begin{aligned} \chi_p'' &\approx 2(1 + 2^{1/(1-p)})^{(1-p)/p} \cdot \chi_\infty'' \quad \text{(in regions I and II)} , \\ \chi_p'' &\approx 2^{1/p} \chi_\infty'' \quad \text{(in regions IIIA and IIIB)} . \end{aligned} \tag{61}$$

The ratio of factors $2(1 + 2^{1/(1-p)})^{(1-p)/p}$ and $2^{1/p}$ in eqs. (60) and (61) ranges from 1 to 1.2 for different values of p. One may therefore conclude that different metrics D_p produce similar chirality maps.

2.4.3. Symmetry of the union of enantiomorphs in their optimum superimposition

Substitution of eqs. (19)–(21) into eq. (3) gives D_p as a function of parameters L, θ, and θ' (see fig. 10). Differentiation with respect to these parameters leads to the following set of equations for the optimum superimposition of class III:

$$\begin{aligned} &(d_A^{p-2} + d_B^{p-2})ab \sin(\gamma + \theta + \theta') + d_A^{p-2} L a \sin\theta \\ &\quad + d_B^{p-2} L b \sin(\gamma + \theta) = 0 , \end{aligned} \tag{62}$$

$$\begin{aligned} &(d_A^{p-2} + d_B^{p-2})ab \sin(\gamma + \theta + \theta') + d_A^{p-2} L b \sin(\gamma + \theta') \\ &\quad + d_B^{p-2} L a \sin\theta' = 0 , \end{aligned} \tag{63}$$

$$\begin{aligned} &d_A^{p-2}[L + b\cos(\gamma + \theta') + a\cos\theta] + d_B^{p-2} \\ &\quad \times [L + b\cos(\gamma + \theta) + a\cos\theta'] + L^{p-1} = 0 . \end{aligned} \tag{64}$$

Subtraction of eq. (63) from eq. (62) yields

$$b[d_B^{p-2} \sin(\gamma+\theta) - d_A^{p-2} \sin(\gamma+\theta')] + a[d_A^{p-2} \sin\theta - d_B^{p-2} \sin\theta'] = 0. \quad (65)$$

$\theta = \theta'$ is an obvious solution of eq. (65) and corresponds to a superimposition with axial symmetry.

2.4.4. Optimum superimposition for class III

With $\theta = \theta'$ eqs. (62) and (63) reduce to eq. (24), and eq. (64) transforms into

$$2d_A^{p-2}[L + b\cos(\gamma+\theta) + a\cos\theta] + L^{p-1} = 0,$$

which, with eq. (19) in mind, gives

$$2\{a^2 + b^2 + L^2 + 2ab\cos(\gamma+2\theta) + 2L[b\cos(\gamma+\theta) + a\cos\theta]\}^{p/2-1}$$

$$\times [L + b\cos(\gamma+\theta) + a\cos\theta] + L^{p-1} = 0. \quad (66)$$

Eq. (24) can be used to express L in terms of θ:

$$L = -\frac{2ab\sin(\gamma+2\theta)}{b\sin(\gamma+\theta) + a\sin\theta}. \quad (67)$$

Substitution of eq. (67) into eq. (66) gives a rational equation in tan θ. The optimum θ thus found, through eqs. (67), (19)–(21) and then (3), determines the exact solution for D_p^{IIIA}. Similarly one can find an exact solution for D_p^{IIIB}.

3. Chirality measures χ'_p of the first kind

Given a normalized triangle, its chirality measure χ'_p of the first kind is defined, according to eq. (4), as the global minimum of function (3), calculated at the optimum superimposition of this triangle and an optimum achiral reference object. It should be noted that although the same functions (3) and (4) are used in the definitions of measures of the first and second kind, a major difference between them makes the definition of χ'_p less transparent: not only relative position, but also the shape and size of an achiral reference object are to be optimized in measures of the first kind, while they are perfectly defined in measures of the second kind where the enantiomorphous triangle serves as the reference object.

An easy solution derives from the fact that, as demonstrated in section 2, the optimum superimposition of enantiomorphous triangles is axially symmetric. This can be used to construct achiral reference objects for chirality measures χ'_p of the first kind and to relate these measures to the corresponding measures χ''_p of the second kind. In order to do that, one needs to relate minimum values $\mathcal{D}_p^i$ (first kind) and D_p^i (second kind) of distance function D_p (eq. (3)) for different classes (i = I, II, III) of optimum superimpositions. The procedure is straightforward for class III: one chooses the midpoints of links between neighboring vertices of enantiomorphs ABC and $A'B'C'$ and joins them together to form the achiral triangle $A^\circ B^\circ C^\circ$ (fig. 12). Obviously, an achiral superimposition of enantiomorphs can be restored from

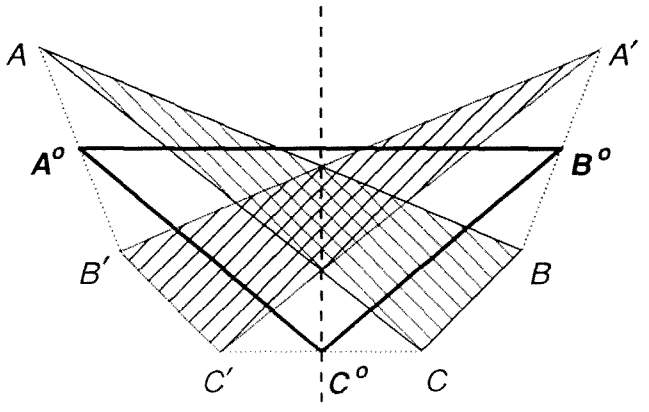

Fig. 12.

a given superimposition of a chiral triangle ABC and an achiral triangle $A^\circ B^\circ C^\circ$ by simple reflection with respect to the symmetry axis of $A^\circ B^\circ C^\circ$. It follows immediately from this construction and from eq. (3) that the minimum distances for the optimum superimpositions in class III are related by

$$\mathcal{D}_p^{\mathrm{III}} = \tfrac{1}{2}\mathrm{D}_p^{\mathrm{III}} . \tag{68}$$

A similar procedure can be applied to the optimum superimpositions in class II. In this case, however, the symmetry axis passes through the midpoints of links AA', BB' and CC', (see fig. 2) and hence the achiral reference object is a degenerate triangle represented by the sequence $A^\circ B^\circ C^\circ$ of three collinear points. Here again, as in the case of class III

$$\mathcal{D}_p^{\mathrm{II}} = \tfrac{1}{2}\mathrm{D}_p^{\mathrm{II}} . \tag{69}$$

The situation is quite different in the case of the optimum superimpositions in class I, where the achiral reference object is merely the line segment AA' (see fig. 1). This segment may be considered as a degenerate isosceles triangle, with the base shrunken into point A'. Obviously, here

$$\mathcal{D}_p^{\mathrm{I}} = \mathrm{D}_p^{\mathrm{I}} . \tag{70}$$

It follows from eqs. (69) and (70), and eqs. (58) and (59) that

$$\mathcal{D}_p^{\mathrm{I}} / \mathcal{D}_p^{\mathrm{II}} \geqslant a/h_C > 1 .$$

Hence,

$$\mathcal{D}_p^{\mathrm{I}} > \mathcal{D}_p^{\mathrm{II}} . \tag{71}$$

This means that χ_p', as the *global* minimum of $\mathcal{D}_p^{\mathrm{i}}$'s, will never equal the minimum distance $\mathcal{D}_p^{\mathrm{I}}$ in class I. As a result, region I does not appear in the chirality map for this kind of measure.

A schematic sketch of the chirality map for measures of the first kind, χ_p', is displayed in fig. 13. As shown by comparison with fig. 7, region I in fig. 7 is split among regions II, IIIA, and IIIB in fig. 13; consequently there is only one triple point T' for measures of the first kind. At the same time, according to (68) and (69), χ_p'' in regions II, IIIA, and IIIB of fig. 7 equals χ_p' multiplied by a constant factor of 2. In the region bordered by dashed lines in fig. 13, which correspond to the boundary lines of region I in fig. 7, $\chi_p''/\chi_p' < 2$. Accordingly, T', which represents the most chiral triangle in terms of χ_p', is located within the borders of the dashed lines and is shifted downward along the IIIA/IIIB boundary line, relative to T. *The shape of the most chiral triangle therefore depends on whether the measure is of the first or of the second kind (see table 1).*

It should be noted that the choice of a degenerate triangle as the achiral reference object is unavoidable since otherwise the whole of region II disappears from the chirality map of fig. 13. Were this to occur, the two remaining regions, IIIA and IIIB, would spread all the way to the x axis, the points of which represent degenerate triangles. The most chiral triangle is represented by the point of intersection of the IIIA/IIIB boundary line with the x axis: a paradoxical result since a degenerate triangle is obviously achiral.

Finally, we emphasize that the technique derived in section 2 for chirality measures of the second kind, after minor modifications, applies equally to measures of the first kind.

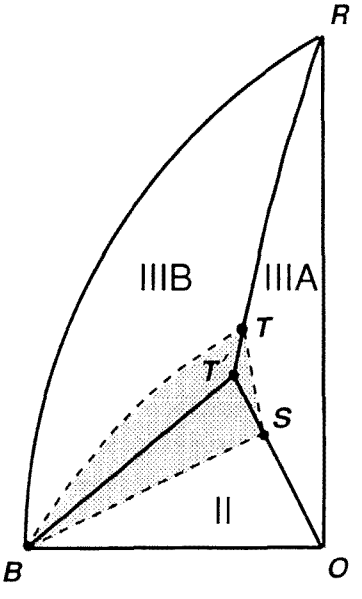

Fig. 13.

4. Concluding remarks

Computational studies of the Hausdorff chirality measure had shown [1,2] that, within the error limits of the calculations, the union of enantiomorphous triangles and tetrahedra is achiral under conditions of maximal overlap. In the present study we have presented analytical proof that under these conditions the union of enantiomorphous triangles is strictly achiral for the general case of a family of measures associated with topologically equivalent metrics, including the special cases of Hausdorff and Euclidean chirality measures. Giering [5] had previously proven that the normalized area of intersection resulting from the overlap of two enantiomorphous triangles (taken as non-empty sets) in E^2 is maximal only if their intersection is achiral. In light of these various findings, and on the reasonable assumption that our analysis and Giering's, though applied to triangles, is valid also for objects of higher dimensions, we believe that there now exists strong evidence for our conjecture [1] that *the union (and hence the intersection) of any object or set and its mirror image is achiral under conditions of maximal overlap.*

The present study reveals that the different chirality measures of a given kind yield similar shapes for the extremal member of the set, i.e., for the most chiral triangle, but that this shape differs significantly for the two kinds of measure (table 1). We emphasize that *none of these measures yields extremal triangles that are degenerate*; this is in contrast to other, previously investigated chirality functions, both of the first [4,6] and the second [7] kind, where the most chiral triangle was found to be infinitely flat, i.e., arbitrarily close to a line segment. Behavior of this type, in which a lowering of dimensionality occurs at the boundary of the shape space, renders the measure unsuitable in any applications to the natural sciences; in that sense the corresponding chirality functions are not well-behaved.

A final remark pertains to the question raised by Fowler [8] on how one "can link the continuous symmetry measure" developed by Zabrodsky et al. [9] "to the study of chirality measures" [1]. The answer is that the "continuous chirality measure" suggested by Zabrodsky et al. is a Euclidean measure of the first kind, χ_2', and, together with the Hausdorff measure χ_∞'' [1,2], constitutes a particular case of the general family of chirality measures χ_p.

Acknowledgements

We thank the Natural Sciences and Engineering Research Council of Canada and the National Science Foundation (U.S.A.) for support of this work, Saul Wolfe for his hospitality, and A.B. Buda for calculating the density plot in fig. 9.

References

[1] A.B. Buda, T. Auf der Heyde and K. Mislow, Angew. Chem. Int. Ed. Engl. 31 (1992) 989.
[2] A.B. Buda and K. Mislow, J. Amer. Chem. Soc. 114 (1992) 6006.

[3] C.G. Pitts, *Introduction to Metric Spaces* (Oliver & Boyd, Edinburgh, 1972).
Yu.A. Shreider, *What is Distance?* (The University of Chicago Press, 1974).
[4] A.B. Buda, T.P.E. Auf der Heyde and K. Mislow, J. Math. Chem. 6 (1991) 243.
[5] O. Giering, Elem. Math. 22 (1967) 5.
[6] T.P.E. Auf der Heyde, A.B. Buda and K. Mislow, J. Math. Chem. 6 (1991) 255.
[7] A.B. Buda and K. Mislow, Elem. Math. 46 (1991) 65;
A.B. Buda and K. Mislow, J. Mol. Struct. (Theochem) 232 (1991) 1.
[8] P.W. Fowler, Nature 360 (1992) 626.
[9] H. Zabrodsky, S. Peleg and D. Avnir, J. Amer. Chem. Soc. 114 (1992) 7843.